Formation of an amorphous product phase during the solid state reaction between a vitreous SiO$_2$ thin film and a (001) BaTiO$_3$ substrate

St. Senz [a], A. Graff [a], D. Hesse [a,*], H.-P. Abicht [b]

[a]*Max-Planck-Institut für Mikrostrukturphysik, Weinberg 2, D-06120 Halle, Germany*
[b]*Fachbereich Chemie, Martin-Luther-Universität Halle-Wittenberg, Kurt-Mothes-Str. 2, D-06120 Halle, Germany*

Abstract

The solid state chemical reaction of a thin SiO$_2$ film with a single-crystal (001) BaTiO$_3$ substrate has been investigated as a model system for processes occurring during the sintering of BaTiO$_3$ ceramics with the sintering additive SiO$_2$. Thin amorphous SiO$_2$ films on (001) BaTiO$_3$ substrates react with the substrate during annealing at 1000°C for 5 to 15 min. Transmission electron microscopy (TEM) has revealed the formation of a glassy reaction product after 5 min of heating. The composition of this glass has been analyzed by energy dispersive X-ray spectrometry (EDX), showing mainly SiO$_2$ and about 16 at.% of BaTiO$_3$. The Ba:Ti ratio of the glass is 1:1. During prolonged heating, or if the initial BaTiO$_3$ surface is decorated with Pt markers, the reaction product crystallizes, with the fresnoite Ba$_2$TiSi$_2$O$_8$ forming as the dominant crystalline phase. © 2000 Elsevier Science Ltd. All rights reserved.

Keywords: BaTiO$_3$; Electron microscopy; Films; Glass; Reaction sequence; SiO$_2$

1. Introduction

Liquid phase sintering has become a common technique, offering the advantages of a decreased sintering temperature, a better development of the microstructure and a larger reproducibility. Of the numerous additives creating liquid phases silica, besides titania, is one of the most important sintering aids for BaTiO$_3$.[1–4] If the additive SiO$_2$ is used to sinter BaTiO$_3$, the lowest melting point in the Ba–Ti–Si–O system is around 1250°C; thus rapid sintering at temperatures below the sintering temperatures of pure BaTiO$_3$ (melting point 1625°C) becomes possible.

A homogeneous distribution of the additive in the grain boundaries is essential. The grain size distribution can be influenced by rapidly growing grains which form in places where the concentration of the additive is high.[2] To improve the homogeneity of the microstructure after sintering, new techniques have been developed to coat each grain of the green body uniformly before sintering.[3] The coating can be performed by spray hydrolysis or by an emulsion technique.[4] For the hot pressing of BaTiO$_3$ ceramics at 1350°C, the initial densification has been described as a grain boundary sliding process promoted by the presence of a viscous grain boundary phase.[5] A Ba-rich composition retards the densification, whereas a Ti-rich composition enhances it. The phase diagram of BaO–TiO$_2$[6] shows the formation of a liquid phase above 1332°C for Ti-rich BaTiO$_3$. On the other hand, Ba-rich BaTiO$_3$ (in thermal equilibrium) consists of Ba$_2$TiO$_4$ and BaTiO$_3$ with a higher melting temperature (> 1560°C).

As shown by Abicht et al.,[4] the highest densification rate in the system BaTiO$_3$–SiO$_2$ occurs between 1100 and 1200°C, i.e. well below the temperature range where a liquid appears (> 1250°C). This densification is perhaps to be attributed to the existence of an amorphous grain boundary phase. Thin intergranular amorphous films have been reported for a SiO$_2$ film deposited on a single-crystal TiO$_2$ substrate[7] and for chlorine-doped silicon nitride ceramics.[8]

The present paper describes a model experiment to study some of the processes occurring during the sintering of BaTiO$_3$ with the sintering additive SiO$_2$. For the work, (001) BaTiO$_3$ single crystals are covered with thin films of SiO$_2$ before they are annealed to induce

---

* Corresponding author. Tel.: +49-345-5582-741; fax: +49-345-5511-223.

E-mail address: hesse@mpi-halle.de (D. Hesse).

solid state reactions. The product phases are then investigated by X-ray diffraction[9] and transmission electron microscopy.

2. Experimental

SiO_2 films of 100 nm in nominal thickness are electron-beam deposited onto well-polished (001) $BaTiO_3$ single crystal surfaces. During deposition, the crystals are heated to 500°C to enhance the adherence of the film. During deposition the oxygen pressure is kept at 10^{-2} Pa by introducing additional oxygen through a needle valve. In some samples, the original $BaTiO_3$ surface is marked by small crystals of Pt, the $BaTiO_3$ crystal being first covered with a Pt film of a few nanometers in thickness at room temperature. Heating at 900°C in air results in a coagulation of the Pt film into small islands. Subsequently, the marked surface is covered with a SiO_2 film as described above.

The oxygen content of the film has not been determined. In general, the oxygen content of amorphous SiO_x films can vary within a wide range, viz. from $SiO_{0.9}$ to $SiO_{2.25}$ depending on the deposition conditions.[10] As can be deduced from Ref. 11, under our deposition conditions, the dominant molecular species in the gas phase are SiO, SiO_2 and O_2. Since surplus O_2 is added through the needle valve, the composition of our films is certainly close to SiO_2 (though some small oxygen deficiency cannot be excluded). Hence the films are called SiO_2 throughout this paper.

The reaction experiments have been performed in a laboratory furnace in air. The samples were heated to the process temperature of 1000°C at a rate of 20 K/min and kept at a constant temperature for the specified time. Then the furnace was allowed to cool down at an initial cooling rate of 50 K/min. Cross-sections of the annealed samples have been prepared routinely by grinding, polishing and ion beam thinning. A Philips CM20FEG transmission electron microscope equipped with a Noran Ge EDX detector and a Gatan magnetic imaging filter (GIF) has been used for subsequent analyses.

3. Results

Examples of the prepared samples have been heated in air at a temperature of 1000°C for 5, 10, 15, and 30 min. Fig. 1 shows TEM cross-section bright-field images of a specimen without Pt markers (Fig. 1a, 5 min) and of two specimens with Pt markers (Fig. 1b, 10 min; Fig. 1c, 15 min). The non-marked sample (a) clearly shows a change in the contrast of the glass along a well-defined interface, indicating the presence of elements heavier than Si and O in the darker region. Tilting the specimen in the electron microscope proved that no crystalline

phase had formed: While the substrate contrast changes rapidly, which is usual for a crystalline material, the film is *amorphous*, not showing any change of the image intensity. Prolonged heating for 2 h led to the formation of crystalline fresnoite $Ba_2TiSi_2O_8$, identified by X-ray diffraction.[12] The samples containing a Pt marker show a different behaviour. After only a *short* heating time the Pt markers are located in the middle of a crystalline product phase (Fig. 1b). The latter is covered with unreacted SiO_2. Electron diffraction identified the crystalline phase as fresnoite $Ba_2TiSi_2O_8$. After 15 min of heating at 1000°C (Fig. 1c) the SiO_2 film is consumed by the reaction with the $BaTiO_3$ substrate. The position of the Pt marker in the middle of the product phase confirms that the diffusion processes during the reaction are transporting material in both directions, viz. inward (into the $BaTiO_3$ crystal) and outward (into the SiO_2 film). The relative contribution of both indiffusion and outdiffusion depends on the local conditions. Furthermore, there is a strong diffusion across the substrate surface. The reaction starts from a continuous SiO_2 film and ends with separated islands of fresnoite. After the reaction, the surface of the sample in Fig. 1c is covered with a gold film at room temperature. This gold film proves that the complex morphology of the film surface is not an artefact of thinning. The surface of $BaTiO_3$ on the right of the fresnoite island is about 50 nm below the Pt marker line. In this place, $BaTiO_3$ seems to be removed and to be transported to the remaining fresnoite islands owing to surface diffusion. Since originally, the SiO_2 film covered the whole surface, Si–O must have also been transported across the surface. The size of the fresnoite grains increases during prolonged annealing. While most of the Pt grains shown in Fig. 1c are embedded into one large fresnoite grain, the fresnoite grains in Fig. 1b are smaller. The reason for this different growth behaviour might be that the Pt islands are acting as nucleation sites for the formation of crystalline product phases. Initially, a large number of small fresnoite grains starts to grow at the (nucleation-promoting) Pt surfaces. Prolonged heating makes them recrystallize into larger fresnoite grains. X-ray diffraction of the Pt-marked reaction films shows the strongest lines of $Ba_2TiSi_2O_8$ (fresnoite) after 10 min of heating only. The sample heated for 30 min additionally contains well-oriented, topotaxially formed Ti-rich phases like $Ba_4Ti_{13}O_{30}$. The Ti-rich phases grow with a direct contact interface to the $BaTiO_3$ substrate.[12] They are located below the Pt marker line.

The chemical composition of the glassy product phase shown in Fig. 1a is determined by an EDX line scan (shown in Fig. 3). The Ba and Ti reference spectra supplied from the EDX software as well as an experimental spectrum of the $BaTiO_3$ substrate are depicted in Fig. 2. The strongest lines, i.e. Ba $L\alpha1$ (at 4.466 keV) and Ti $K\alpha$ (at 4.509 keV) overlap due to the limited EDX
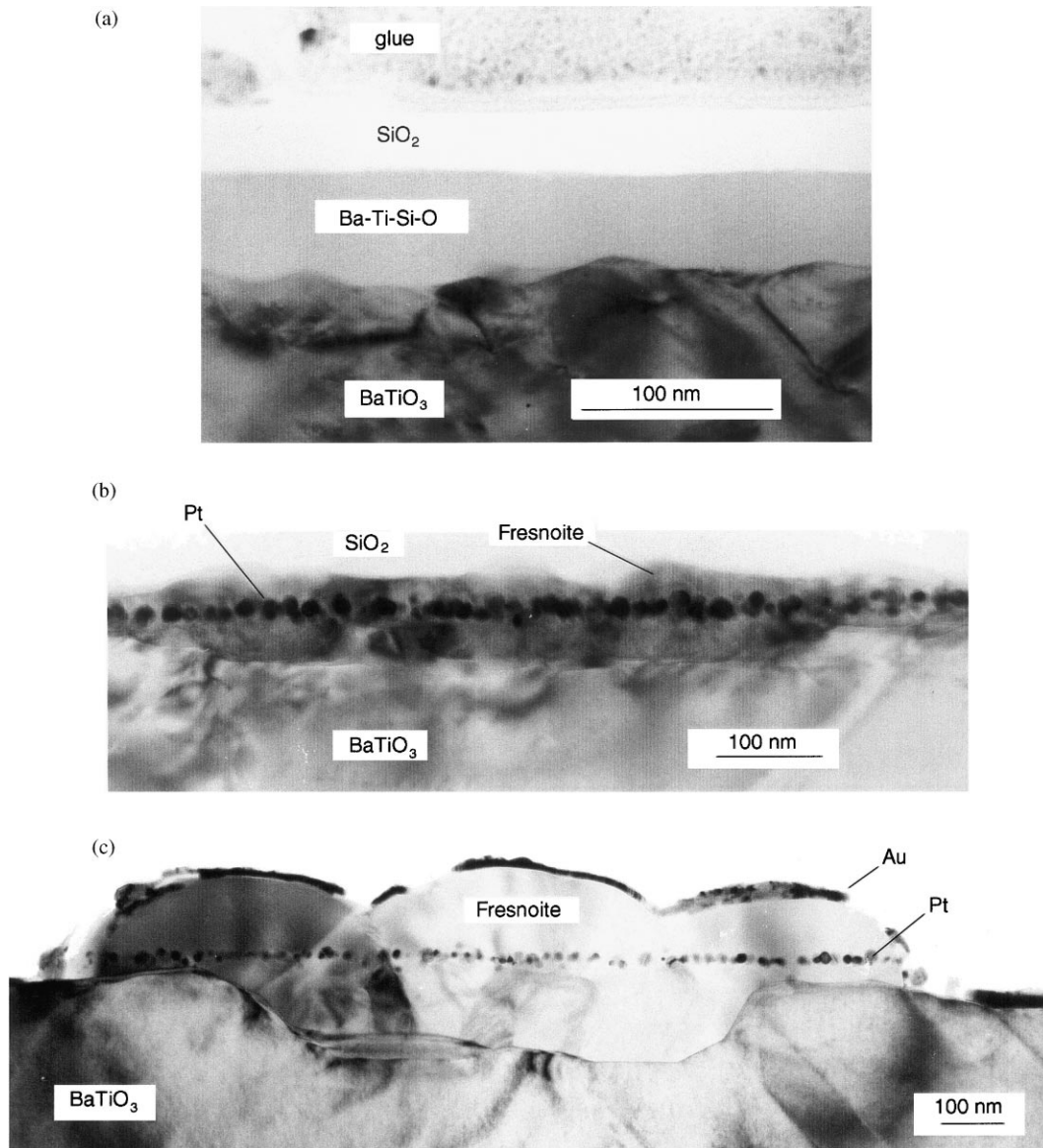
Fig. 1. TEM bright-field images of amorphous SiO_2 films after the reaction with a $BaTiO_3$ substrate at 1000°C: (a) 5 min, (b) 10 min, with Pt marker, (c) 15 min, with Pt marker.

energy resolution of about 140 eV (Fig. 2). (The spectra have been normalized with respect to the amplitude of the strongest line.) Fortunately, the Ba L spectrum also contains a series of weaker lines with higher energies, which do not overlap with the Ti $K\alpha$ and $K\beta$ lines.

The line scan software offers pre-defined channels centred around the strongest line of the element chosen. In the following, these pre-defined channels are marked by brackets [ ], while the physical X-ray lines are indicated by plain letters. Since the Ba-to-Ti concentration ratio cannot be determined from the intensities of the respective physical X-ray lines due to the above-mentioned overlap, this ratio has to be obtained in a more indirect way, viz. from the different X-ray intensities falling into some of the pre-defined channels. Due to their position with respect to the Ba_L and Ti_K reference spectra, the pre-defined

channels $[Ba_L + Ti_K]$, $[Ce_L]$ and $[Nd_L]$ turned out to be suitable, as shown in Fig. 2, with the lower and upper edges of each of these three pre-defined channels indicated by broken lines.

Indeed, the ratio of Ba to Ti can approximately be obtained from the following three channels: (i) $[Ba_L + Ti_K]$ ranging from 4.40 to 4.58 keV and covering the physical X-ray lines Ba $L\alpha1$ (4.466 keV) and Ti $K\alpha1$ (4.509 keV), (ii) $[Ce_L]$ ranging from 4.76 to 4.89 keV and covering the physical X-ray lines Ba $L\beta1$ (4.828 keV) and Ti $K\beta1$ (4.932 keV), and (iii) $[Nd_L]$ ranging from 5.16 to 5.28 keV covering *only* the physical X-ray line Ba $L\beta2$ (5.156 keV). Comparing the intensity of the $[Ba_L + Ti_K]$ channel with that of the $[Ce_L]$ and $[Nd_L]$ channels approximately reveals the Ba to Ti ratio in the glass as, for instance, the $[Nd_L]$ channel does not include
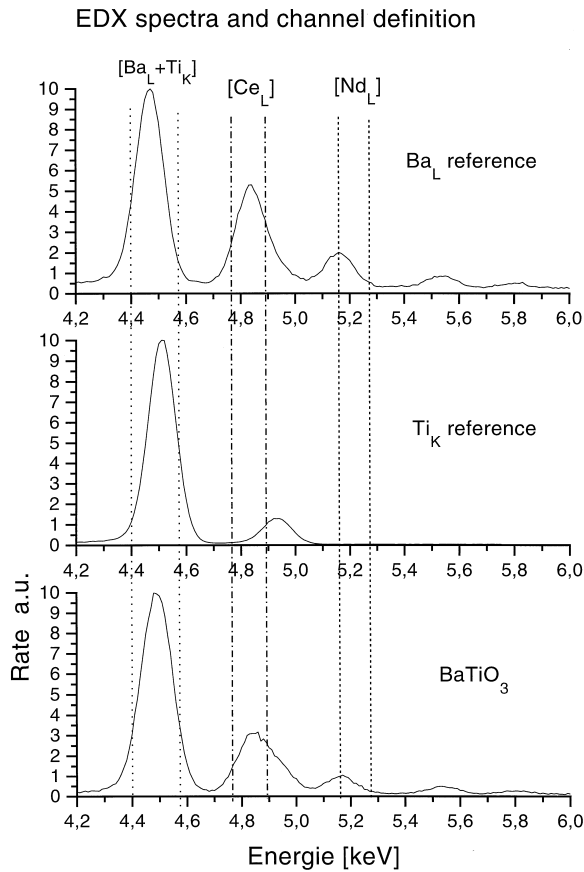
EDX spectra and channel definition

Fig. 2. Ba-L and Ti-K EDX reference spectra with overlapping lines, experimental BaTiO$_3$ substrate spectrum, and definition of the three pre-defined channels used for the line scans.

Fig. 3. EDX line scans across an amorphous SiO$_2$ film after the reaction with the BaTiO$_3$ substrate for 5 min at 1000°C. The scan started in the BaTiO$_3$ substrate (left). One step corresponds to a distance of 14

a titanium signal (for details see below). Fig. 3 shows line scans and calculated ratios of the channels [Ba$_L$ + Ti$_K$], [Nd$_L$] and [Ce$_L$], corresponding to the lines of higher energy, as well as the [Si$_K$] channel. The relative contribution of Ba and Ti to the three channels varies: Ba lines fall into all of the channels, whereas Ti is strong only in the [Ba$_L$ + Ti$_K$] channel, weak in the [Ce$_L$] channel and absent in the [Nd$_L$] channel. Thus the ratio of the weaker [Ce$_L$] and [Nd$_L$] channels to the [Ba$_L$ + Ti$_K$] channel implies some information about the element ratio Ba:Ti. Within the limits set by the statistical noise the ratio Ba:Ti does not change on moving from BaTiO$_3$ to the glassy product phase, i.e. the Ba:Ti ratio in the reacted glass is also about 1. From the change of the signal of the [Ba$_L$ + Ti$_K$] channel at about 4.5 keV and the change of the [Si$_K$] channel at 1.74 keV the molar ratio of (Ba plus Ti) to Si in the glassy product phase can be estimated at 15–18 mol%.

Though the oxygen O$_K$ line at 525 eV overlaps with the Ti$_L$ lines at 452 and 458 eV, the oxygen signal can be used to monitor the specimen thickness, because it dominates the intensity of the overall line formed by the overlap. Hence, the specimen proved to be quite flat, because scanning from the BaTiO$_3$ substrate into the
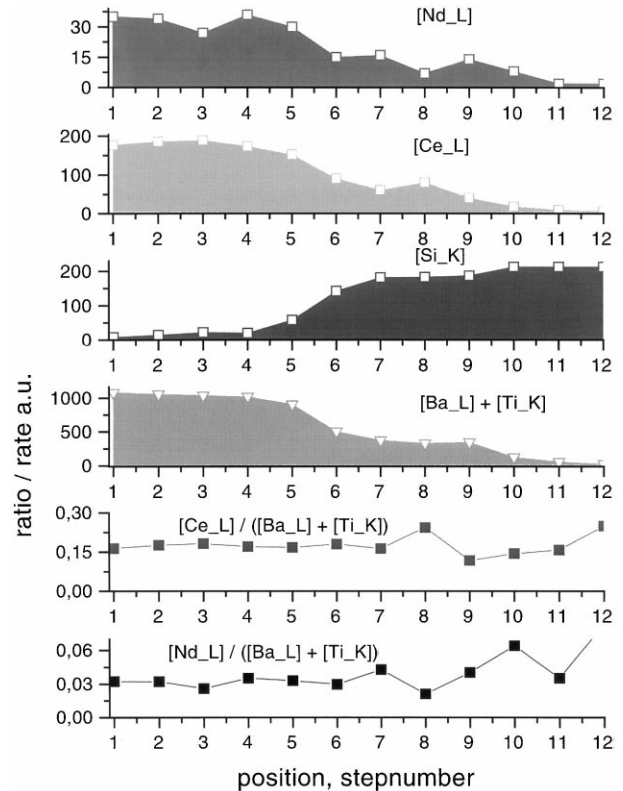
glass (not shown here) yielded a constant oxygen count rate. Only the upper part of the non-reacted SiO$_2$ film is wedge-shaped.

4. Discussion

The discussion is divided into three parts. The first and second parts are concerned with our two main observations of (i) the formation and subsequent crystallization of a metastable Ba-Ti-Si-O glass during the reaction of a BaTiO$_3$ crystal with a SiO$_2$ film at 1000°C, and (ii) the fact that the element distribution in this glass is flat, i.e. the diffusion profiles of Ba and Ti in the reacted glass are identical in the limits of our experimental resolution. The third part discusses (iii) the influence of the above glass (and similar ones) on the densification of the ceramics at the initial stage of sintering.

(i). The formation of bulk samples of Ba–Ti–Si–O glass from oxide and carbonate precursors as well as their properties have been investigated by several authors. After Köppen and Dietzel, the melting temperature of Ba–Ti–Si–O glasses shows a flat minimum (≈1250°C) for Ba/Ti/Si compositions close to 25/25/50 at.%.[13] A glass with a lower content of Ba and Ti, viz. 16.6/16.6/66.6%, melts only at about 1600°C.[13] Ba–Ti–Si–O glasses are metastable and can be heated for some time

before they start to crystallize. The crystallization of fresnoite $Ba_2TiSi_2O_8$ from glasses has been studied before with the aim to produce ultrasonic transducers consisting of a glass ceramic[14] and also to obtain pyro-electric glass ceramics.[15] Heating a glass of the composition of 18% BaO, 18% TiO_2 and 64% SiO_2 at a rate of 10 K/min revealed an exothermic crystallization peak at 860°C. Yamauchi et al. proved that a thin film was amorphous that had been obtained by sputtering a stoichiometric $Ba_2TiSi_2O_8$ target at substrate temperatures lower than 170°C.[16] The film was poor in Ba, i.e. rich in Ti. The activation energy for the crystallization of the film was 370 kJ/mol. While heated at 850°C for up to 30 min, the film remained amorphous during an X-ray diffraction measurement. However, after 75 min of heating, sharp crystalline fresnoite reflections occurred. All these observations explain the crystallization of our Ba–Ti–Si–O glass after prolonged heating reasonably well.

In general, a reaction process resulting in a crystalline product phase requires the formation of a nucleus of a size above a critical minimum value. In our case, the reaction between the $BaTiO_3$ substrate and the amorphous SiO_2 film can, however, proceed without any nucleation, because the initial phase is amorphous, as is the intermediate product phase. A similar, even stronger preference of a glassy product phase is known from solid state amorphization: Two crystalline metals can react to form an intermediate glassy product phase, which crystallizes only upon prolonged annealing. In this case, too, the formation of the crystalline product phase is delayed because of the nucleation. In our system, one of the reactants is a glass, and the reaction at the SiO_2/Ba–Ti–Si–O interface can be considered a dissolution of Ba and Ti ions into the SiO_2 glass. As discussed below, the diffusion of the *network modifier* Ba^{2+} into the SiO_2 glass is certainly faster, whereas the Ti^{4+} ions should move more slowly owing to their *network-preserving* character and their higher charge. The necessity that both Ba and Ti ions dissolve into the glass determines the time evolution of the reaction. From the concentrations measured of Ba and Ti in the glass, which are rather low compared to the composition of the crystalline product phase $Ba_2TiSi_2O_8$, it can be concluded that the solubility of Ba and Ti in SiO_2 is limited. Both ions are metastable in a SiO_2 glass: at higher concentrations crystalline precipitates are formed, viz. barium silicate and TiO_2 precipitates.

After the reaction, the surface of the $BaTiO_3$ substrates shows a lateral waviness of several hundred nanometer in wavelength. Since the surface had initially been flat this waviness can be interpreted to result from the reaction partly propagating also into the $BaTiO_3$ substrate. To elucidate this, the marker experiment has been performed, with a different reaction occurring, however: the product phase now immediately crystallizes, and the marker shows that the reaction proceeds now in both directions, viz. into the substrate and into the SiO_2

film. If the SiO_2 film is grown on top of a thin Pt layer, the surface of the Pt grains offers nucleation sites of a high density. Thus the product phase immediately crystallizes, with a polycrystalline film of fresnoite forming.

ii. The observed fact, according to which the Ba-to-Ti ratio in the glassy product phase is close to one, deserves a detailed discussion, because the diffusion coefficients of Ba^{2+} and Ti^{4+} in SiO_2 are certainly different. As will be explained below, the former fact may be understood as the result of concentration-dependent diffusion coefficients.

The Ba^{2+} and Ti^{4+} ions differ in their behaviour in the SiO_2 glass matrix: Si^{4+} can be replaced by Ti^{4+} without the need to break the network, whereas Ba^{2+} is a network modifier. In their study of Ti–Si–O glasses, Henderson and Fleet showed that low concentrations of Ti are indeed incorporated into the network of the glass, with Ti^{4+} being four-fold coordinated by oxygen.[17] Higher Ti concentrations resulted in a modified neighbourhood of Ti, with a mixture of four- and five-fold coordination occurring. A partial replacement of Si by Ti has also been observed in the crystalline solid solution $Ba_2Ti_{1+x}Si_{2-x}O_8$ ($0 < x < 0.14$).[18] Infra-red spectra proved that the excess Ti is indeed tetrahedrally coordinated in this substituted fresnoite crystal.

Contrary to Ti^{4+}, Ba^{2+} does not fit into the network of the glass and locally changes the network into a state of weaker bonding. In such a glass of modified structure, the ions diffuse certainly faster than in a pure SiO_2 glass. Accordingly, the diffusion coefficient of barium $D_{Ba} = f_1 (c_{Ba}, c_{Ti})$ increases with the Ba content c_{Ba} in the glass, at least for low concentrations. As a consequence, Ti should now also move faster in the Ba-modified glass: $D_{Ti} = f_2(c_{Ba}, c_{Ti})$. As a result, the titanium diffusion front is coupled to the barium front, which is the first precondition for the observed Ba-to-Ti ratio being close to one. Another prerequisite is that the solubilities of Ba and Ti, that depend on the respective concentrations and on temperature, are similar. Since these dependencies are not known, only a general shape of the functions can be used to interpret the element profile in the product phase as follows.

The reaction of $BaTiO_3$ and SiO_2 can be considered an indiffusion of Ba and Ti ions into the SiO_2 glass matrix. In the literature, there are no results providing quantitative data about the simultaneous indiffusion of Ba^{2+} and Ti^{4+} into a SiO_2 glass. *Self-diffusion* experiments of pure SiO_2 show a relatively high activation energy. The activation energy for *viscous flow* in pure SiO_2 glass is 6 eV,[19] which is identical with the activation energy of 6 eV of the self-diffusion of Si in vitreous glass.[20] The Si diffusion in β-quartz along the c-axis has an activation energy of 7.6 eV,[21] similar to the above values of the glass. Remarkably, the activation energies for the Si self-diffusion and viscous flow in pure SiO_2 glass were thus found to be similar at temperatures between 1180 and 1400°C, which is above the glass temperature T_g

($\approx$1200°C) of SiO_2. At these temperatures, SiO_2 has a high viscosity of the order of 10^{10} to 10^{12} Pa·s. The viscosity can be reduced by introducing network modifiers: A glass with SiO_2, Al_2O_3, MgO, and CaO as its main constituents (called a haplobasaltic silicate melt) has a viscosity of the order of only 1 Pa·s around 1400°C.[22] The activation energies of the self-diffusion of several elements (Ba^{2+}: 181 kJ/mol, Ti^{4+}: 206 kJ/mol) in this haplobasaltic silicate melt were similar to that of the viscous flow in the melt. The diffusion coefficients depended on the ionic radius and charge only weakly, decreasing by a factor of ten from Mg^{2+} to $U^{5+/6+}$. This correspondence of the activation energies of diffusion and viscosity over several orders of magnitude of the viscosity is valid only for ions that are incorporated into the network of the glass. Strong network modifiers like alkali elements, for instance, diffuse in a different way. Since the above silicon self-diffusion data for pure SiO_2 had been measured above the glass temperature T_g, a diffusion temperature higher than the glass temperature seems to be necessary for a close relation between the activation energies of diffusion and viscosity.

Assuming that the diffusion in our silica-based glass proceeds via a mechanism obeying this relation, the increase of the diffusion coefficients can be described by the decrease of viscosity as soon as the network modifier Ba^{2+} is added to the SiO_2 glass. Moreover, the glass temperature T_g decreases as soon as network modifiers are introduced. (For example, T_g of a glass of 35.7 mol% BaO and 64.3 mol% SiO_2 is low, viz. near 700°C.[23]) After the reaction, the glass in our film contains about 8% BaO and 8% TiO_2 so that most probably, T_g of this glass is below the reaction temperature of 1000°C. Thus, for our films the Ba^{2+} and Ti^{4+} diffusion can be considered a process with an activation energy similar to that of viscous flow. Compared to pure SiO_2 glass, the viscosity of our Ba–Ti–Si–O glass is certainly several orders of magnitude lower, the diffusivities of Ba and Ti being considerably higher.

The mean diffusion coefficient D of Ba and Ti in the Ba–Ti–Si–O glass can be estimated from the observed width of the reaction zone x after time t from the relation $x^2 = D \cdot t$. With $x = 50$ nm and $t = 300$ s it follows that $D = 8 \times 10^{-18}$ m²/s. Of course, this estimation at the best presents the order of magnitude of the diffusion coefficient, because the real processes cannot be modelled by applying Fick's first law. A better description would require the knowledge of other terms like the interface-flux resistance and the integration of concentration-dependent diffusion coefficients.

Quantitatively, the self-diffusion of network formers in a glass melt is described by the Eyring equation. It relates the diffusion coefficient D to the viscosity η: $D = k \cdot T/(\eta \cdot \lambda)$; k is the Boltzman constant and λ the diffusional jump distance. Using the diameter of an oxygen anion (0.27 nm) as an estimate of λ and the

above-estimated diffusion coefficient D results in the viscosity $\eta \approx 8 \times 10^6$ Pa·s at 1000°C. This estimated value of the viscosity is of the same order of magnitude as that of 10^5 Pa·s of a glass containing 35.7 mol% BaO and 64.3 mol% SiO_2 at 1000°C extrapolated from measurements around 750°C.[20] The glass formed in our thin film contained fewer network modifiers, thus probably implying a slightly higher viscosity. Hence, the simultaneous in-diffusion of the network modifiers Ba^{2+} and Ti^{4+} into SiO_2 showing a viscosity of $\eta \approx 10^7$ Pa·s seems to fulfil the Eyring equation, which originally had been established for the self-diffusion of network formers in a highly polymerized melt.

iii. The sintering of $BaTiO_3$ ceramics can be modified by coating the $BaTiO_3$ grains with a sintering aid prior to sintering. Abicht et al.[4] compared the compaction of green bodies with coatings of Ba–Ti–Si–O, Ti–O and Ti–Si–O precursors. All these coatings reduced the activation energy of the initial sintering. Compared to the sintering of pure $BaTiO_3$ the shrinking was faster and occurred at a lower temperature. The time/shrinking exponent during the first 10 min of heating was 1, thus pointing to a viscous mechanism during the initial sintering. The coating was about 10 nm thick, provided it was homogeneous. On the other hand, the experiments described here show the formation of a glassy reaction product during the first minutes of heating. Accordingly, the results of Abicht et al.[4] can be explained by a process similar to that observed in the present work. Since the coatings Abicht et al. used had been produced from precursors at low temperatures, most probably, they were amorphous. The crystallization of these glasses seems to be delayed, just as in our films. As a consequence, the glassy coating reduced the friction forces during the gliding of grains within the first minutes of sintering.

5. Conclusions

A glassy Ba–Ti–Si–O thin-film product phase is forming intermediately during the solid state reaction between an amorphous SiO_2 film and a (001) $BaTiO_3$ single crystal substrate. The incorporation of ions of both different valency (Ba^{2+} vs. Ti^{4+}) and behaviour relative to the network of the glass (network modification vs. preservation) reduces the viscosity of this glassy Ba–Ti–Si–O film as compared to the initial, amorphous SiO_2 film.

This model experiment suggests that, most probably, there is a similar process going on on the surfaces of the individual $BaTiO_3$ grains during the sintering of $BaTiO_3$ electroceramics using the sintering additive SiO_2. Thus the high densification rate Abicht et al. observed at temperatures *well below* the respective eutectic temperatures can now be explained by grain sliding processes made possible by the intermediate formation of a glassy mixed oxide film of low viscosity.

Acknowledgements

References

1. Liu, G. and Rosemann, R. D., Effect of BaO and SiO_2 addition on PTCR $BaTiO_3$ ceramics. *J. Mater. Sci.*, 1999, **34**, 4439.

2. Yoo, Y.-S., Kim, H. and Kim, D.-Y., Effect of SiO_2 and TiO_2 addition on the exaggerated grain growth of $BaTiO_3$. *J. Eur. Ceram. Soc.*, 1997, **17**, 805.

3. Abicht, H.-P., Langhammer, H. T. and Felgner, K.-H., The influence of silicon on microstructure and electrical properties of La-doped $BaTiO_3$ ceramics. *J. Mater. Sci.*, 1991, **26**, 2337.

4. Abicht, H.-P., Völtzke, D. and Schmidt, H., Preparation, characterization and sintering behaviour of barium titanate powders coated with Ba-, Ca-, Si- and Ti-containing compounds. *Mater. Chem. Phys*, 1997, **51**, 35.

5. Mostaghaci, H. and Brook, R. J., Kinetics of hot-pressing of $BaTiO_3$ ceramics. *Brit. Ceram. Trans. J.*, 1985, **84**, 203.

6. Kirby, K. W. and Wechsler, B. A., Phase relations in the barium titanate-titanium oxide system. *J. Am. Ceram. Soc.*, 1991, **74**, 1841.

7. Ackler, H. D. and Chiang, Y.-M., Model experiment on thermodynamic stability of retained intergranular amorphous films. *J. Am. Ceram. Soc.*, 1997, **80**, 1893–2467.

8. Pezzoti, G., Ota, K. and Kleebe, H.-J., Viscous slip along grain boundaries in chlorine-doped silicon nitride. *J. Am. Ceram. Soc.*, 1997, **80**, 2341.

9. Senz, S., Graff, A., Blum, W., Hesse, D. and Abicht, H.-P., Orientation relationships of reactively grown $Ba_6Ti_{17}O_{40}$ and $Ba_2TiSi_2O_8$ on $BaTiO_3$ (001) determined by X-ray diffractometry. *J. Am. Ceram. Soc.*, 1998, **81**, 1317–2220.

10. Sun, Y. N., Feldman, A. and Farabaugh, E. N., X-ray photoelectron spectroscopy of O1s and Si2p lines in films of SiO_x formed by electron beam evaporation. *Thin Solid Films*, 1988, **157**, 351.

11. Lamoreaux, R. H., Hildenbrand, D. L. and Brewer, L., High-temperature vaporization behavior of oxides II. Oxides of Be, Mg, Ca, Sr, Ba, B, Al, Ga, In, Tl, Si, Ge, Sn, Pb, Zn, Cd, and Hg. *J. Phys. Chem. Ref. Data*, 1987, **16**, 419.

12. Senz, S., Graff, A., Blum, W., Abicht, H.-P., & Hesse, D., Formation of fresnoite and Ti-rich phases during the solid state reaction between a $BaTiO_3$ substrate and a SiO_2 film, In *Ceramics getting into the 2000's*, ed. P. Vincenzini. Pt. A. *Advances in Science and Technology, Vol.13. Proc. 9th World Ceramic Congress & Forum on New Materials CIMTEC 1998*, Florence, Italy, 14–19 June 1998. Techna srl Publ., Faenza 1999, pp. 207–214.

13. Köppen, N. and Dietzel, A., Über das System $BaO–TiO_2–SiO_2$. *Glastechn. Ber.*, 1976, **49**, 199(in German).

14. Ting, R. Y., Halliyal, A. and Bhalla, A. S., Polar glass ceramics for sonar transducers. *Appl. Phys. Lett.*, 1984, **44**, 852.

15. Halliyal, A., Bhalla, A. S., Newnham, R. E. and Cross, L. E., $Ba_2TiGe_2O_8$ and $Ba_2TiSi_2O_8$ pyroelectric glass-ceramics. *J. Mater. Sci.*, 1981, **16**, 1023.

16. Yamauchi, H., White, R. J., Ayukawa, M., Murray, T. C. and Robinson, J. W., The structure of thin films sputter deposited from a $Ba_2Si_2TiO_8$ ceramic target. *J. Mater. Res.*, 1988, **3**, 105.

17. Henderson, G. S. and Fleet, M. E., The structure of Ti silicate glasses by micro-Raman spectroscopy. *Canadian Mineralogist*, 1995, **33**, 399.

18. Coats, A. M., Hirose, N., Marr, J. and West, A. R., Tetrahedral Ti^{4+} in the solid solution $Ba_2Ti_{1+x}Si_{2-x}O_8$ $(0 \leqslant x \leqslant 0.14)$. *J. Solid State Chem.*, 1996, **126**, 105.

19. Donnadieu, P., Jaoul, O. and Kléman, M., Plasticité de la silice amorphe de part et d'autre de la transition vitreuse. *Phil. Mag. A*, 1985, **52**, 5(in French).

20. Brebec, G., Seguin, R., Sella, C., Bevenot, J. and Martin, J. C., Diffusion du silicium dans la silice amorphe. *Acta Metall.*, 1980, **28**, 327(in French).

21. Jaoul, O., Béjina, F. and Élie, F., Silicon self-diffusion in quartz. *Phys. Rev. Lett.*, 1995, **74**, 2038.

22. LaTourrette, T., Wasserburg, G. J. and Fahey, A. J., Self diffusion of Mg, Ca, Ba, Nd, Yb, Ti, Zr, and U in haplobasaltic melt. *Geochimica Cosmochimia Acta*, 1996, **60**, 1329.

23. Sridharan, S. and Tomozawa, M., Effect of various oxide additives on sintering of $BaO-SiO_2$ system glass-ceramics. *J. Mater. Sci.*, 1992, **27**, 6747.